Modification and Performance Analysis of a Bidirectional DC-DC Converter with Voltage Gain for the Energy Management of Supercapacitors

Jessica C. A. de Sousa, Thiago. M. Soares, Jonathan M. Tabora, Maria Emília de L. Tostes, José Moisés M. Silva, *and* Hugo G. Lott

Abstract-- **This paper presents modifications and performance analysis of a high voltage gain DC-DC converter topology for energy management in supercapacitor storage systems. Computer simulations were performed using PSIM software in thermal simulation mode, taking into account the real characteristics of the components. The results obtained are close to the real ones, with low voltage and current ripple on the DC bus and passive components, increasing the efficiency of the system with supercapacitors from the modifications made to the bidirectional DC-DC converter topology with high voltage gain.**

Index Terms—**Efficiency; High voltage gain bidirectional DC-DC converters; energy management; storage systems; supercapacitors.**

I. INTRODUCTION

SINCE the Paris Agreement in 2015, the installed capacity of clean renewable energy has grown significantly, driven by government interest and policies aimed at keeping the global average temperature increase below 2°C compared to pre-industrial levels [1], [2].

However, there are isolated communities in Brazil in the Amazon region where fossil fuels usually meet energy needs, causing a significant negative impact on the environment concerning CO_2 emissions.

This situation has motivated the realization of an R&D project with the local utility Norte Energia S. A. to construct and implement a mini-generation plant consisting of a photovoltaic system with a hybrid storage system, that is, an Ion Lithium battery and supercapacitor banks, to reduce or eliminate the diesel generator's participation and thus reduce greenhouse gas emissions.

In addition to battery storage systems, supercapacitors are another energy storage technology increasingly used worldwide, especially in hybrid systems with specific requirements for high discharge power over short periods due to their high power density, low internal resistance, wide operating temperature range, and high efficiency [3].

The operation of these energy storage devices needs the use of bidirectional power converters for controlling the amount of energy during their charge and discharge process, which has triggered the growing interest in studies related to converter topologies as it can be observed through a bibliometric review performed on the Scopus platform. For this purpose, a single string with the word "DC-DC converter topologies" was performed, which resulted in 1159 documents related to DC-DC converters and their different applications in power systems. Figure 1 depicts the number of studies dealing with DC-DC converter topologies over the last 24 years. The countries leading the publications based on the search performed are India, the United States, China, and Canada, with almost half of the studies.
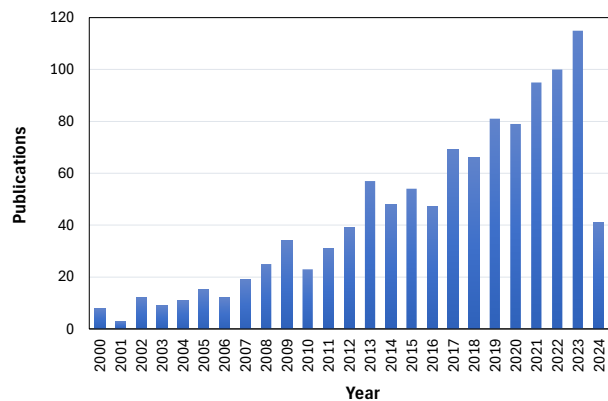
Fig. 1. Publications per year associated with DC-DC converter topologies.

The type of DC-DC converter used depends on the application and can be isolated or non-isolated. In the literature, isolated topologies include flyback, half-bridge, and full-bridge

Jessica C.A.de Sousa (e-mail: jessicacristina13@gmail.com), Thiago M. Soares (e-mail: thiagosoares@ufpa.br), Maria Emília de L. Tostes (e-mail: tostes@ufpa.br) are with the Amazon Energy Efficiency Center, Federal University of Pará, Belém, PA, Brazil.

Jonathan M. Tabora (e-mail: jonathan_mt24@hotmail.com) is with the Electrical Engineering Department, National Autonomous University of Honduras, UNAH, Tegucigalpa, F.M., Honduras.

José Moisés M. Silva (e-mail: josemachado@norteenergiasa.com.br), and H. G. Lott (e-mail: hugolott@norteenergiasa.com.br), are with Norte Energia S.A.

XV LATIN-AMERICAN CONGRESS ON ELECTRICITY GENERATION AND TRANSMISSION - CLAGTEE 2024
Mar del Plata, Argentina, November 27th – 29th, 2024

2

converters, mainly used for charging and discharging uninterruptible power supply (UPS) batteries. Among the non-isolated topologies, conventional buck-boost, multilevel, trilevel, switched capacitor, Sepic/Zeta, and coupled inductor converters stand out, mainly for applications such as power systems, electric mobility, etc., and depending on the topology used, it is possible to obtain low levels of current ripple in the inductors and low levels of voltage ripple in the capacitors to reduce the stress on the conductors [4], [5], [6].

Some authors have applied this solution to power systems, such as [7], who proposed a hybrid system consisting of a diesel engine and a supercapacitor and used an interleaved bidirectional buck-boost converter to convert energy between the supercapacitor and the DC bus. In his thesis, [8] proposed using a bidirectional buck-boost converter and supercapacitors for a system to increase the power of electric vehicles. In his work, [9] presented the implementation of an autonomous photovoltaic system using supercapacitors as an energy storage unit, where a bidirectional buck-boost converter provides the connection between the DC bus and the supercapacitor.

The paper in [13] analyzes an electric vehicle configuration based on supercapacitors and batteries for energy transfer, and the power flow between the energy sources and the vehicle is through a DC bus connected to an interleaved bidirectional DC-DC converter. By facilitating the bi-directional flow of energy, these converters enable the integration of diverse energy sources and storage systems, including renewable energy sources such as solar and wind, as well as battery and supercapacitor storage. This capability enhances the reliability and resiliency of microgrids, allowing them to operate independently of the main grid during outages or periods of high demand, supporting more sustainable and robust energy systems.

Considering the growth of renewable energy in recent years and the emergence of new technologies and categories, such as electric vehicles and hybrid microgrids, the use of storage solutions is becoming more relevant in national and international contexts. This article evaluates DC-DC converter topologies for supercapacitor power management based on computational simulations performed in the PSIM software. For the simulations, real characteristics of the components were considered from the software's thermal simulation mode, thus allowing the monitoring of semiconductor losses and results closer to the real ones.

The topologies include the bidirectional buck-boost DC-DC converter topology and a new interleaved bidirectional buck-boost topology with high voltage gain presented by [11].

- Verify the performance of the modifications made to the high voltage gain topology in systems with supercapacitors;
- Verify the performance of topologies for supercapacitor system applications.

II. THEORETICAL FOUNDATION

A. Supercapacitors

Supercapacitors store energy as an electric field between two conductive plates. These plates are typically coated with activated carbon, which offers a high surface area, excellent electrical conductivity, chemical inertness, and relatively low cost. A separator material is placed between the two conductive plates to prevent direct electronic contact between the electrodes while allowing the free flow of anions and cations. The assembly of electrodes and the separator are immersed in a highly conductive electrolyte [6], [12]. Compared to lithium-ion batteries, supercapacitors have a high-power density, which allows for fast charging and discharging, but if not coupled together, they have a low energy density. The analogy of energy density and power density between electrochemical batteries, supercapacitors, and capacitors is illustrated in Fig. 2.
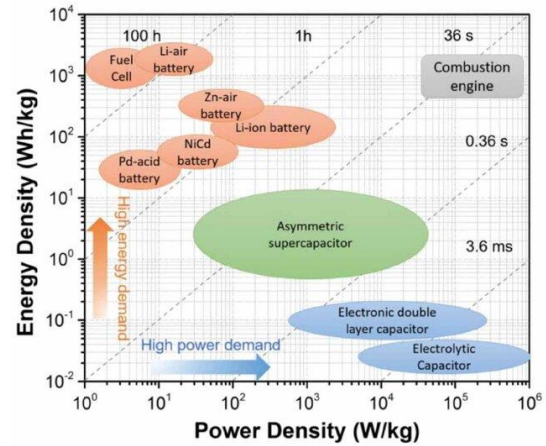
Fig. 2. Specific power vs specific energy Ragone plot for different electrical energy-storage technologies [13].

Supercapacitor performance is largely attributed to the properties of the activated carbon coating, which maximizes the surface area for storing charge. The separator increases the efficiency and safety of the energy storage process by providing ionic conductivity while maintaining electrical isolation between the electrodes. The combination of these components makes supercapacitors suitable for applications ranging from renewable energy systems to electric vehicles by enabling high power density, fast charge/discharge cycles, and long operating life [14], [15].

A supercapacitor storage system consists of supercapacitors, a bi-directional DC-DC converter, and a power source; it may also use another storage solution or power device to form a hybrid storage system. In some configurations, the system may consist only of supercapacitors and the DC-DC converter. The DC-DC converter is key to providing greater controllability and flexibility to the system, allowing efficient management of the energy flow in both directions.

For computational analysis, PSIM adopts the equivalent macro-electrochemical model of supercapacitors presented in its manual [16]. The schematic is illustrated in Fig. 3.
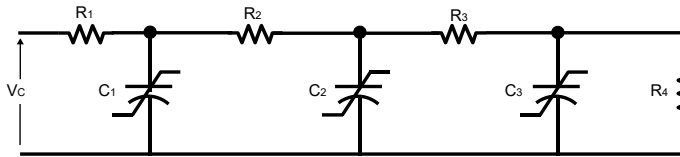
Fig. 3. Equivalent electrochemical model of supercapacitors considered with PSIM software.

The supercapacitor is a nonlinear device, and in this model, its capacitance depends on the voltage applied to the terminals [16], according to (1). The supercapacitor's nonlinearity curve is shown in Fig. 4.

$$C(V_C) = C_O + K_V V_C \qquad (1)$$

where C_O is the initial linear capacitance, representing the capacitor's electrostatic capacitance, K_V is a positive coefficient that reflects the change in capacitance with voltage, and V_C is the applied voltage.
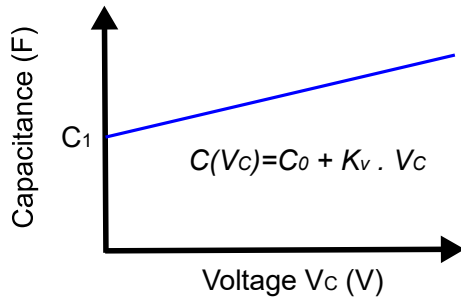
Fig. 4. Capacitance control from the voltage.

To determine the model for the charging and discharging behavior in PSIM simulations, information from the data sheet and experimental measurements of the supercapacitor are needed [16]. The graph in Figure 5 shows some of these parameters.
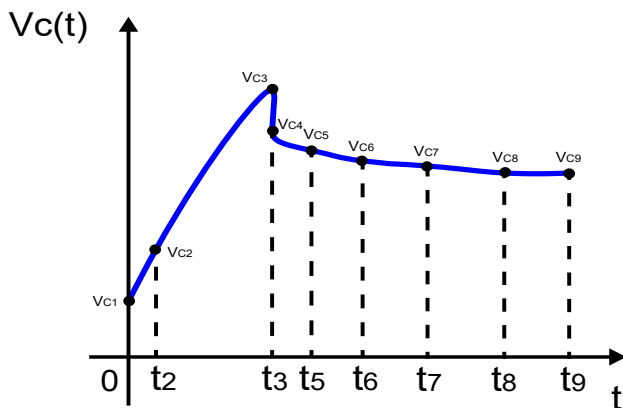
Fig. 5. Supercapacitor charging and discharging parameters.

B. DC-DC Converters

The main characteristic of bidirectional DC-DC converters is the power flow between two sources in both directions, as shown in Figure 6. The operation of the semiconductor defines the concept of bidirectional power flow switches that allow current to flow in both directions. For this particular study, one

of the sources is the supercapacitor, and the other is the 48 V DC bus.
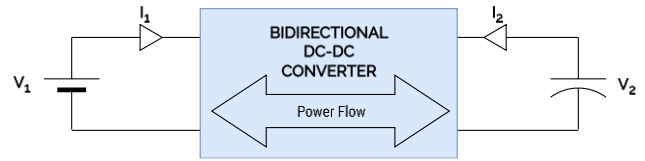
Fig. 6. Power flow between two sources in bidirectional converters.

The non-isolated topology commonly used in supercapacitor bank storage systems is the bidirectional buck-boost topology, which is derived from the unidirectional buck-boost topology by replacing the diode with a semiconductor switch, as shown in Figure 7 [17].
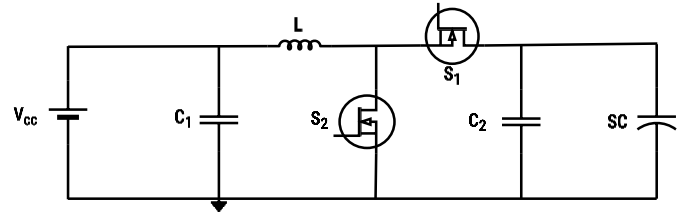
Fig. 7. Conventional Bidirectional Buck-Boost Converter.

C. Bidirectional DC-DC Converter with High Voltage Gain

The author in [11] presents a non-isolated, interleaved, high-gain DC-DC converter topology consisting of four sets of semiconductor switches and diodes (S1, S2, S3, and S4), two inductors, and three capacitors. In each direction, two switches are used as power switches, while the other two are used as synchronous rectifiers. This converter's high gain is more suitable than the conventional bidirectional buck-boost converter. The converter proposed by [11] is shown in Fig. 8.
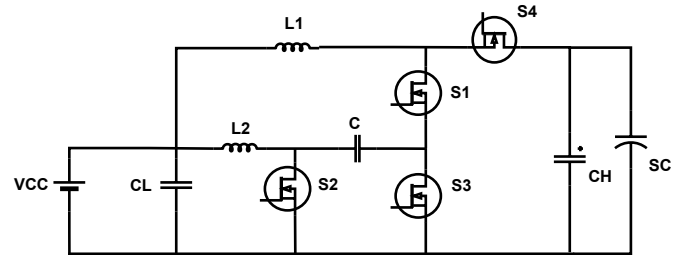
Fig. 8. Bidirectional DC-DC converter with high voltage gain.

In step-down mode, switches S3 and S4 act as power switches, while S1 and S2 act as synchronous rectifiers. In boost mode, switches S1 and S2 act as power switches, and switches S3 and S4 act as synchronous rectifiers.

Based on an analysis of electrical circuits, [11] defines that the static gain for the voltage step-down mode and the voltage step-up mode are respectively:

$$\frac{V_{CC}}{V_{SC}} = G_{VCCM\ (Buck)} = D^2 \qquad (2)$$

$$\frac{V_{SC}}{V_{CC}} = G_{VCCM\ (Boost)} = \frac{1}{(1-D)^2} \qquad (3)$$

where D is the cyclic ratio.

The minimum inductance values for the voltage step-down mode can be seen in (4) and (5).

$$L_1 \geq \frac{(1 - D^2)R_L}{2D^2 f_s} \qquad (4)$$

$$L_2 \geq \frac{R_L}{2f_s} \qquad (5)$$

where f_s is the switching frequency and R_L is the DC bus resistance.

For voltage boost mode, the minimum inductance values are:

$$L_1 \geq \frac{D(2 - D)(1 - D)^2 R_L}{2f_s} \qquad (6)$$

$$L_2 \geq \frac{(1 - D)^4 R_L}{2f_s} \qquad (7)$$

For boost mode operation, resistance R_L corresponds to the equivalent series resistance of the supercapacitor.

Finally, the central capacitor is determined by (8).

$$C \geq \frac{1}{\Delta V_C}(1 - \sqrt{\frac{V_L}{V_H}})\sqrt{\frac{V_L}{V_H}\frac{P_o}{V_L}} \qquad (8)$$

D. Modified High Voltage Gain Bidirectional DC-DC Converter

In order to improve the converter presented by [11] for application in supercapacitor storage systems, some modifications are being proposed in this study. As shown in Fig. 9, two new inductors (L1' and L2') have been added in parallel to the existing inductors, L1 and L2. In addition, a capacitor C' has been added in series with the central capacitor C. The aim of these proposed modifications to the DC-DC converter with high voltage gain is to reduce losses, reduce the high current flow over the inductors, reduce ripple over the inductors and central capacitor and increase the converter's output efficiency
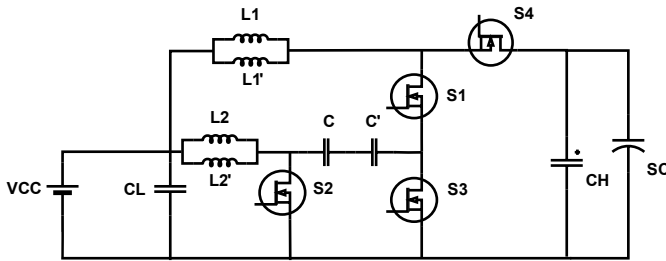
Fig. 9. Bidirectional DC-DC Converter with Modified High Gain Voltage

Mathematically, $L_1 = L_1'$ and $L_2 = L_2'$, then the inductance values for the voltage step-down mode are equivalent to (9) and (10):

$$L_1 = L_1' \geq 2 \times (\frac{(1 - D^2)R_L}{2D^2 f_s}) \qquad (9)$$

$$L_2 = L_2' \geq 2 \times (\frac{R_L}{2f_s}) \qquad (10)$$

And for the voltage elevator mode, the inductances are equivalent to (11) and (12):

$$L_1 = L_1' \geq 2 \times (\frac{D(2 - D)(1 - D)^2 R_L}{2f_s}) \qquad (11)$$

$$L_2 = L_2' \geq 2 \times (\frac{(1 - D)^4 R_L}{2f_s}) \qquad (12)$$

The central capacitors can be expressed as in the previous section because their values are the same.

III. RESULTS DISCUSSION

To validate the assumptions of this study, a series of simulations were performed on the converters in the PSIM software using the specifications in Table I. The semiconductor model used is the silicon carbide MOSFET. The 48 V DC bus is supplied by a 62 F - 162 V supercapacitor module. The power transfer between the sources is 20 kW.

TABLE I
DESIGN PARAMETERS AND SPECIFICATIONS AND COMPONENTS

Parameters	Specifications
Rated Voltage of SC	V_{SC} = 162 V
DC bus voltage rating	V_{CC} = 48 V
Rated output power	Po = 20 kW
Switching frequency	f_s = 500 kHz
Ripple current on the inductors	ΔI_L = 0,1% I_L
DC bus ripple voltage	ΔV_{CC} = 2% V_{CC}
Semiconductor switches	MOSFET's IMW120R007M1H
Central capacitors and output capacitive filters	01 10 μF/250 V parallel-connected aluminum electrolytic capacitor (ESG106M250AH4AA/KEMET) 02 aluminum electrolytic capacitors connected in series of 500 μF/250 V (MLPS501M250EA0C/CDE) 02 x 2.2 mF/250 V parallel-connected aluminum electrolytic capacitors (B43630E2228M000/EPCOS)

A. Project Inductance Selection

The choice of inductances is an extremely important point for the project, as they define the conduction mode and current ripple in the converter. Therefore, in addition to the calculations made using the equations presented, it was considered as a design criterion that the ripple should be minimal, in this case 0.1% of IL or close to that value. For this analysis, some simulations were carried out to observe the behavior of the inductors when discharging the supercapacitor. For the L1 inductor of the converter proposed by [11] and for the set of inductors (L1 and L1') of the modified converter, the behavior of the values shown in Table II was observed in the simulation.

TABLE II
INDUCTANCE VALUES FOR INDUCTORS L1

	Buck-Boost Converter with High Voltage Gain (L1)	Modified High Voltage Gain Buck-Boost Converter (L1 and L1')
Inductances	0,2736 µH	0,5472 µH
	547,42 µH	1094,8 µH

Similarly, the same criteria were used for the L2 inductances of the converter proposed by [11] and for the set of inductors (L2 and L2') of the modified converter. Table III shows the values analyzed in the computer simulation.

TABLE III
INDUCTANCE VALUES FOR INDUCTORS L2

	High Voltage Gain Buck-Boost Converter (L2)	Modified High Voltage Gain Buck-Boost Converter (L2 and L2')
Inductance	0,1152 µH	0,2304 µH
	230,76 µH	461,52 µH

When L1 = 0.2736 µH and L2 = 0.1152 µH were considered in the simulation of the converter proposed by [11], it could not be completed because the current in the semiconductor switches and inductor L1 reached high values, causing the software to interrupt the simulation. Meanwhile, the current in inductor L2 reaches values below 0 A. The waveform of the current in inductors L1 and L2 can be seen in Fig. 10.
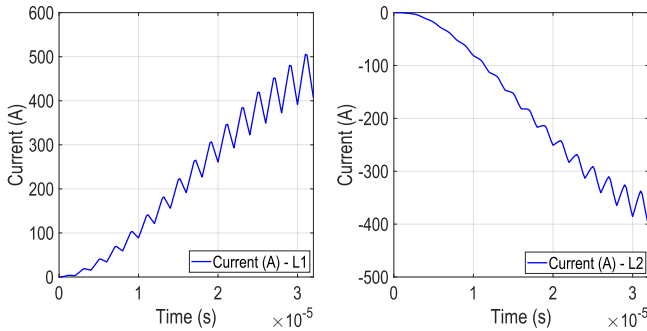
Fig. 10. Waveforms over the inductors when applying L1 = 0.2736 µH (Left) and L2 = 0.1152 µH (right) for the converter proposed by [11].

By simulating L1 = L1'= 0.5472 µH and L2 = L2'= 0.2304 µH for the buck-boost topology with modified high voltage gain, the current is better controlled, but the ripple current through the inductors is too high. In addition, it has been observed that in this case the inductors L2 and L2' operate in discontinuous mode. The behavior of the modified converter in this case is shown in Figure 11.
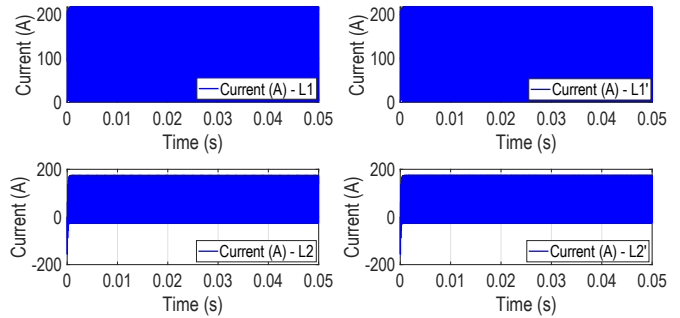
Fig. 11. Waveforms over the inductors when applying L1 = L1' = 0.5472 µH and L2 = l2' = 0.2304 µH in the modified converter.

When using L1 = 0.2736 µH and L2 = 230.76 µH, while the current ripple of inductor L2 reaches the defined design criteria, inductor L1 operates in discontinuous conduction mode and shows high current ripple, as shown in Fig. 12. 12. Similarly, if the values of L1 = 547.42 µH and L2 = 0.1152 µH are considered, the current ripple of the inductor on L1 reaches the values specified for the design, while the inductor L2 operates in discontinuous conduction mode, as shown in Fig. 13.
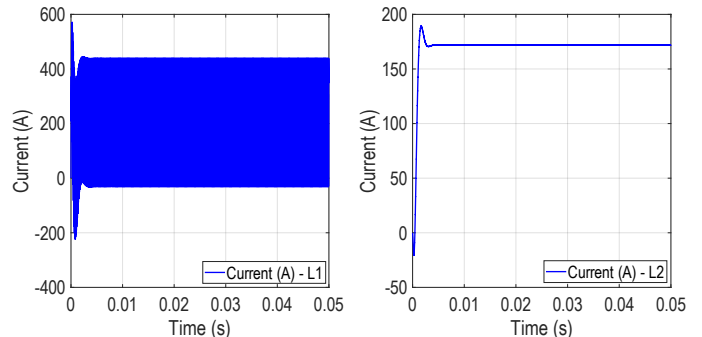
Fig. 12. Waveforms over the inductors when applying L1 = 0.2736 µH and L2 = 230.76 µH to the converter with high voltage gain.
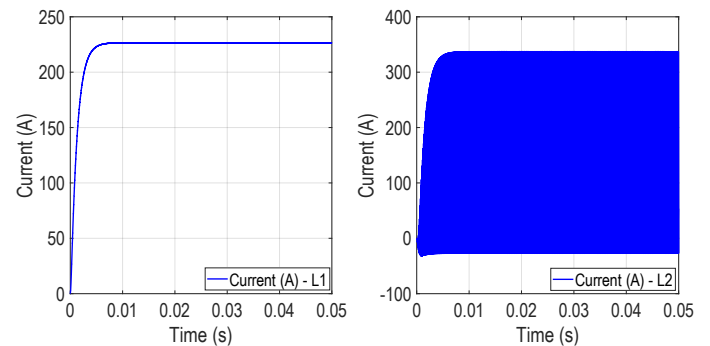
Fig. 13. Waveforms over the inductors when applying L1 = 547.42 µH and L2 = 0.1152 µH to the converter proposed by [11].

When using L1 = L1'= 0.5472 µH and L2 = L2'= 461.52 µH, the inductors L1 and L1' operate in discontinuous mode, while L2 and L2' operate under the conditions previously defined in the design, as shown in Fig. 14. Similarly, when L1 = L1' = 1094.8 µH and L2 = L2' = 0.2304 µH, L2 and L2' operate in discontinuous conduction mode and L1 and L1' operate in the conditions defined in the design, as shown in Fig. 15.

XV LATIN-AMERICAN CONGRESS ON ELECTRICITY GENERATION AND TRANSMISSION - CLAGTEE 2024
Mar del Plata, Argentina, November 27th – 29th, 2024

6
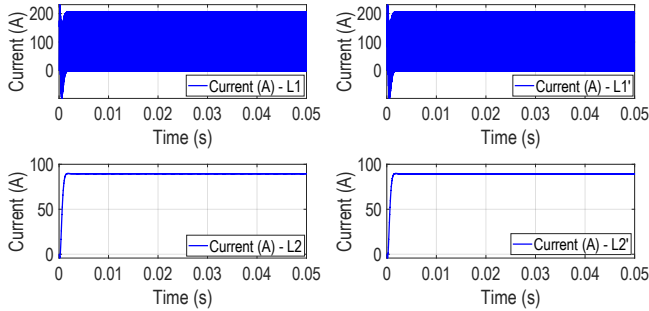
Fig. 14. Waveforms over the inductors when applying L1 = L1' = 0.5472 µH and L2 = l2' = 461.52 µH in the modified converter.
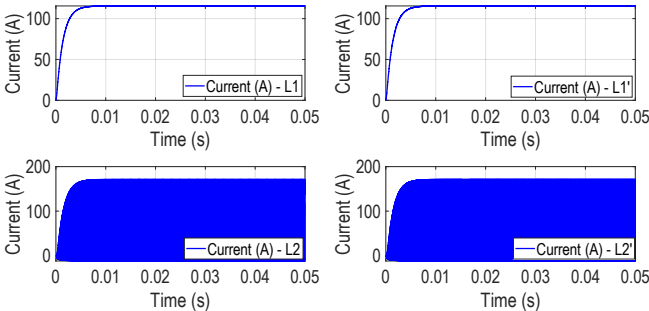
Fig. 15. Waveforms over the inductors when applying L1 = L1' = 1094.8 µH and L2 = l2' = 0.2304 µH to the modified converter.

Considering L1 = 547.42 µH and L2 = 230.76 µH for the converter proposed by [11], it operates within the current ripple values defined in the design and in continuous operation mode, as can be seen in Fig. 16.
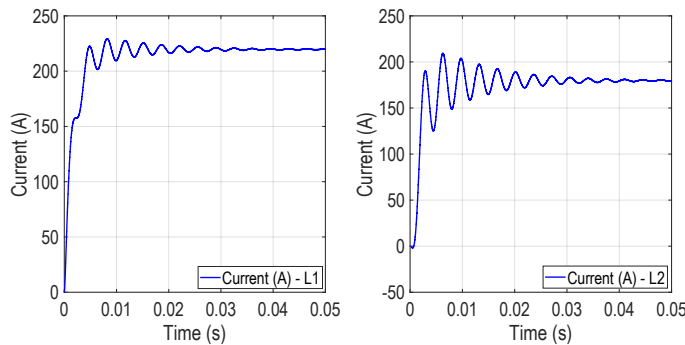
Fig. 16. Waveforms over the inductors when applying L1 = 547.42 µH and L2 = 230.76 µH to the converter proposed by [11].

By using L1 = L1'= 1094.8 µH and L2 = L2'= 461.52 µH in the converter with modified high voltage gain, it works within the ripple values specified in the design in continuous operation mode and at lower current levels compared to the converter proposed by [11], as shown in Fig. 17.
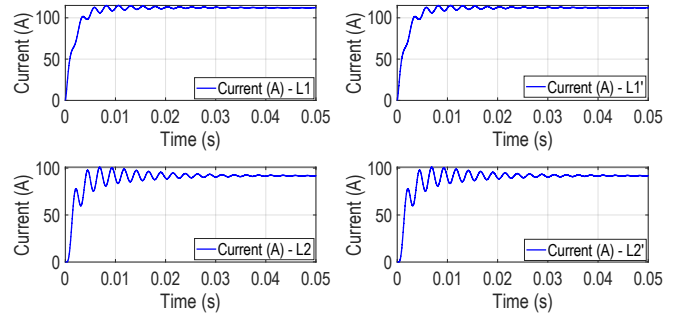
Fig. 17. Waveforms over the inductors when applying L1 = L1' = 1094.8 µH and L2 = l2' = 461.52 µH to the modified converter.

In this case, we can conclude that it is important to pay attention to the choice of the inductor to reduce the stress on the components and the cabling used. In addition, it was possible to observe the effectiveness of the modifications made to the topology of [11] by controlling the current and reducing the level and the ripple of the current on the inductors.

B. Converter output performance

The curves obtained were related to the discharge of the supercapacitor on the DC bus to analyze the performance of the converters. The output voltages of the converters presented in the previous section, the conventional bidirectional buck-boost converter, the bidirectional buck-boost with high voltage gain, and the modified bidirectional buck-boost with high voltage gain, are shown in Fig. 18. Where it can be seen that with the modifications made to the converter proposed by [11], the voltage approaches the nominal value of the DC bus of 48 V, as well as presenting a low voltage ripple on the bus.
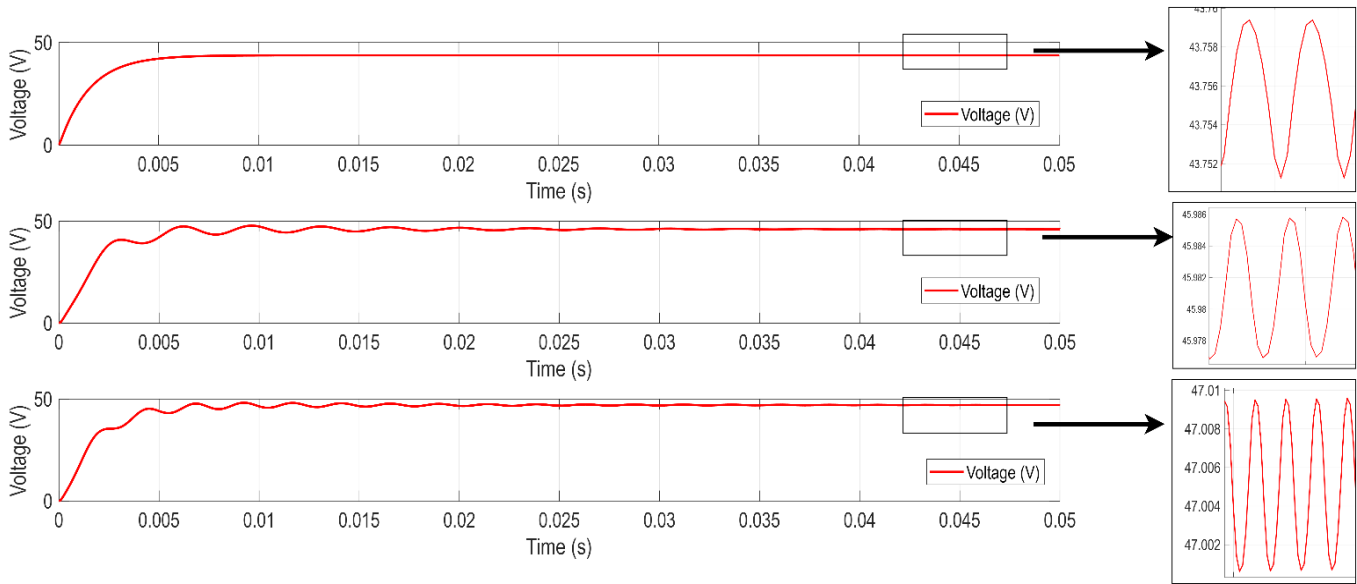
Fig. 18. Output voltage waveforms of the conventional bidirectional DC-DC converter, bidirectional DC-DC converter with high voltage gain, and modified bidirectional converter with high voltage gain.
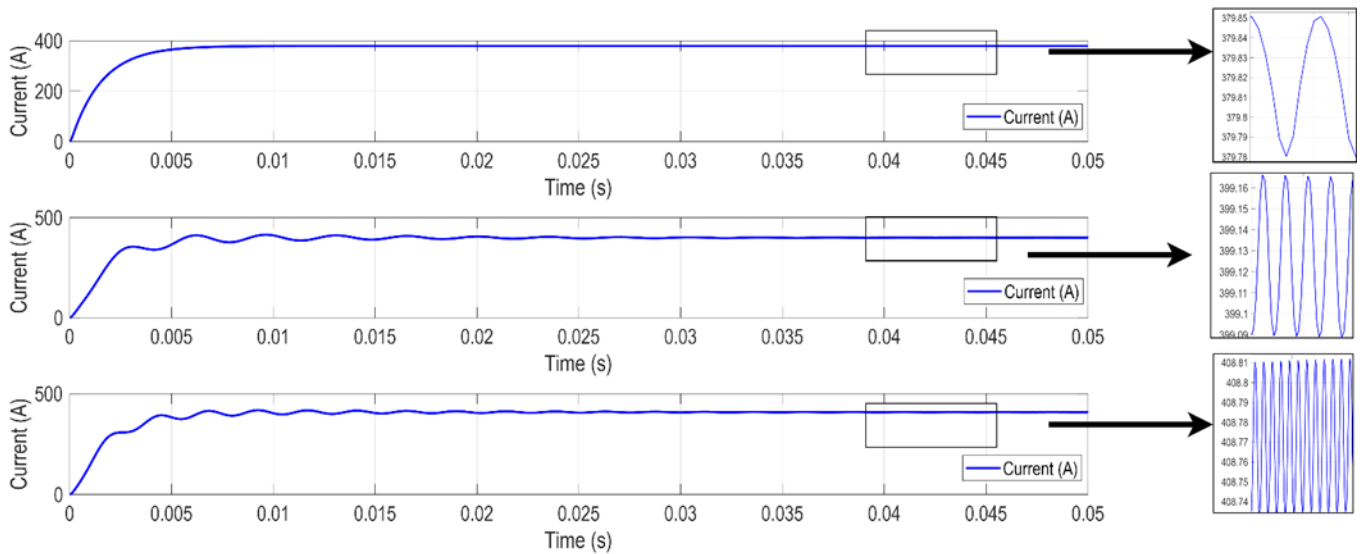
Fig. 19. Output current waveforms of the conventional bidirectional DC-DC converter, bidirectional DC-DC converter with high voltage gain, and modified bidirectional converter with high voltage gain.

XV LATIN-AMERICAN CONGRESS ON ELECTRICITY GENERATION AND TRANSMISSION - CLAGTEE 2024
Mar del Plata, Argentina, November 27th – 29th, 2024

8
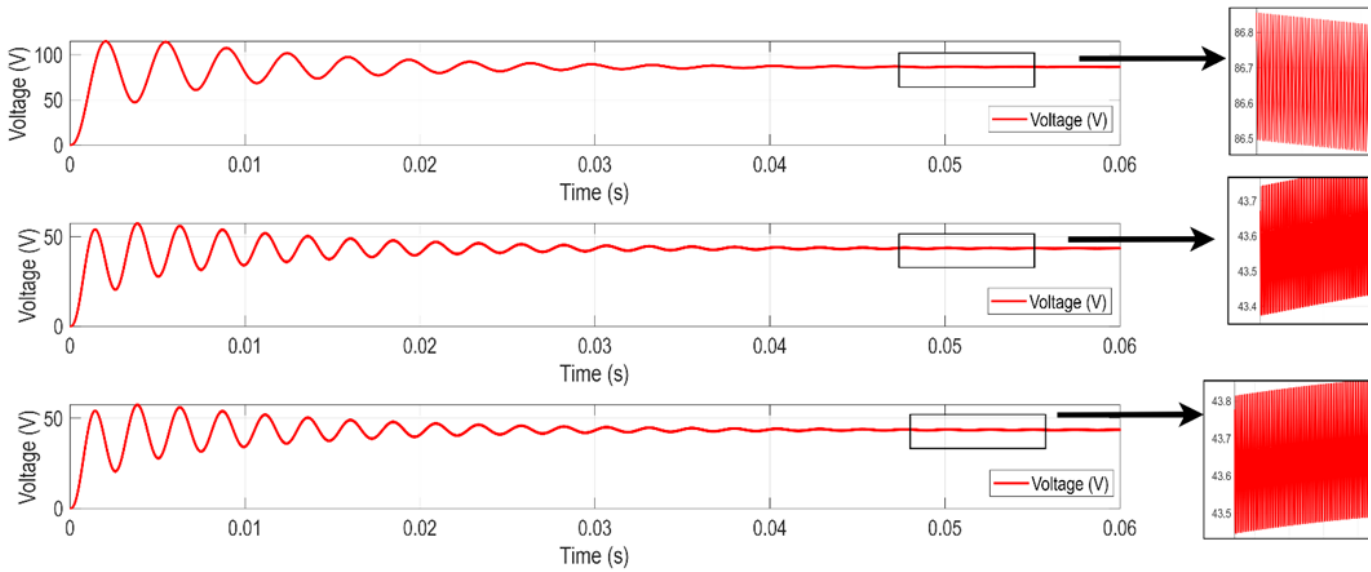
Fig. 20. Waveforms of the voltage on the central capacitor of the bidirectional DC-DC converter with high voltage gain and of the central capacitors C and C' of the modified bidirectional converter with high voltage gain.

Similar to the output voltage, the current on the DC bus increases, as shown in Fig. 19. The proposed topology has a higher current when discharging the supercapacitor, about 408 A, and a ripple of 0.08 A, while conventional bidirectional and high-gain topologies have an output current of about 399 A.

With regard to the central capacitors in the topology proposed by [11] and its modification, Fig. 20 shows a reduction in the stress and ripple on the components. As mentioned in the previous section, switches S3 and S4 operate in voltage step-down mode. Based on the characteristics of the selected MOSFET, the PSIM software obtained the power dissipation curves for the active switches.

Fig. 21 shows the power dissipation curves for the active switches in the topology presented in [11], while Fig. 22 shows the power dissipation curves for switches S3 and S4 in the modified topology. In this case, it is possible to see close loss values in the active semiconductor switches present in the presented topologies.
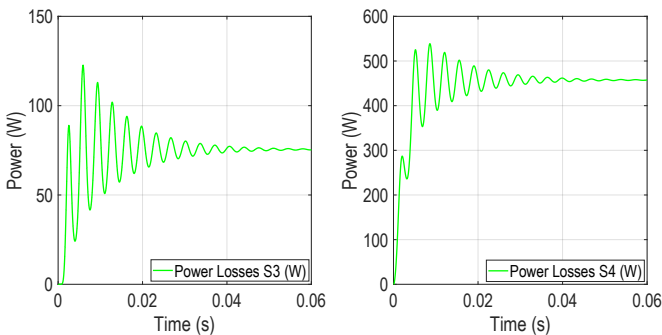
Fig. 21. Power losses on switches S3 e S4 in bidirectional DC-DC converter with high voltage gain.
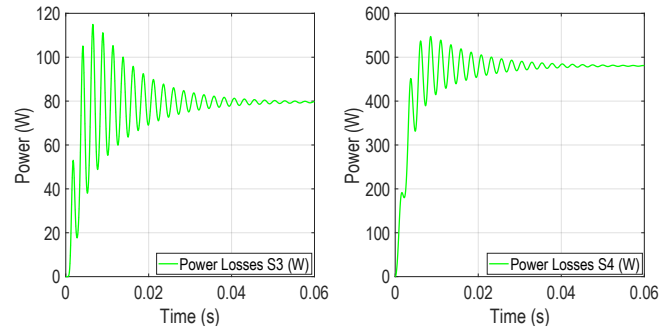
Fig. 22. Power losses on switches S3 and S4 are bidirectional in a modified DC-DC converter with high voltage gain.

Finally, Fig. 23 shows the converters' performance for the application with supercapacitors. The modified converter has a higher power dissipation and, therefore, a higher efficiency, around 96.05%, while the conventional topology has an efficiency of 83% and the topology proposed by [11] 92%. The simulations considered all the losses present in the system, thus validating the efficiency of the proposed modifications for power dissipation using supercapacitors.
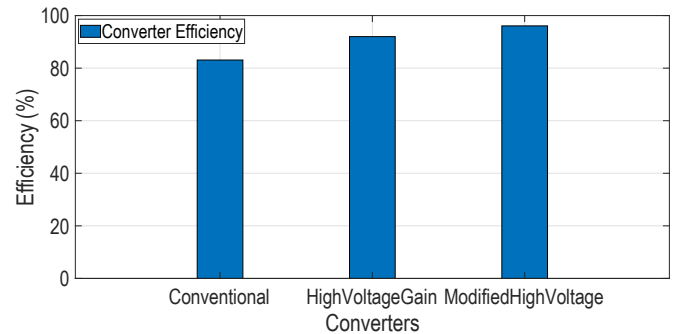
Fig. 23. Efficiency of converters for storage systems with supercapacitors.

IV. CONCLUSIONS

This work focuses on presenting and analyzing the modifications introduced in the topology of the high-

performance bidirectional DC-DC converter proposed by [11] and evaluating its performance when applied to storage systems with supercapacitors.

The improved performance of the modified converter was verified from the results obtained in the computational simulations. The implemented modifications achieved a significant increase in system efficiency and a noticeable reduction in output ripple in both the DC bus and passive components. These improvements demonstrate the feasibility and effectiveness of the modified converter for application in supercapacitor energy storage systems.

In summary, the modifications made not only optimize the converter's performance but also broaden its applicability in the context of advanced storage systems. As future projections, the development of an optimized control technique for these converters is proposed, as well as its experimental implementation to validate the results obtained in the simulation and ensure its performance in real operating conditions.

V. REFERENCES

[1] U. Nations, "Cumbre de las Naciones Unidas sobre el desarrollo sostenible | Naciones Unidas", United Nations. Acesso em: 7 de junho de 2024. [Online]. Disponível em: https://www.un.org/es/conferences/environment/newyork2015

[2] International Energy Agency, "World Energy Outlook 2023 – Analysis", IEA. Acesso em: 29 de junho de 2024. [Online]. Disponível em: https://www.iea.org/reports/world-energy-outlook-2023

[3] E. T. Serra, O. Alcir de Faro, A. Mossé, e N. Martins, "Armazenamento de Energia: Situação Atual, Perspectivas e Recomendações", Fórum de Energias Renováveis de Roraima. Acesso em: 20 de julho de 2024. [Online]. Disponível em: https://energiasroraima.com.br/armazenamento-de-energia-situacao-atual-perspectivas-e-recomendacoes/

[4] J. Wang, B. Wang, L. Zhang, J. Wang, N. I. Shchurov, e B. V. Malozyomov, "Review of bidirectional DC–DC converter topologies for hybrid energy storage system of new energy vehicles", *Green Energy Intell. Transp.*, vol. 1, nº 2, p. 100010, set. 2022, doi: 10.1016/j.geits.2022.100010.

[5] R. Mayer, A. Péres, e S. V. Oliveira, "CONVERSOR CC-CC MULTIFÁSICO BIDIRECIONAL EM CORRENTE NÃO ISOLADO APLICADO A SISTEMAS ELÉTRICOS DE TRAÇÃO DE VEÍCULOS ELÉTRICOS E HÍBRIDOS. (MULTIPHASE BIDIRECTIONAL DC/DC NON-ISOLATED CONVERTER FOR ELECTRIC DRIVE SYSTEM IN ELECTRIC VEHICLE AND HYBRID ELECTRIC VEHICLE)", *Rev. Interam. Radiol.*, vol. 20, ago. 2015.

[6] A. A. Ferreira e J. A. Pomilio, "Estado da Arte sobre a Aplicação de Supercapacitores em Eletrônica de Potência", *Eletrônica Potência*, vol. 10, nº 2, Art. nº 2, nov. 2005, doi: 10.18618/REP.2005.2.025032.

[7] S.-M. Kim e S.-K. Sul, "Control of Rubber Tyred Gantry Crane With Energy Storage Based on Supercapacitor Bank", *IEEE Trans. Power Electron.*, vol. 21, nº 5, p. 1420–1427, set. 2006, doi: 10.1109/TPEL.2006.880260.

[8] F. Lium, "30 kW Power Boost System for Drive Trains for Electric Vehicles Based on Supercapacitor Technologies", Master thesis, Institutt for elkraftteknikk, 2007. Acesso em: 21 de julho de 2024. [Online]. Disponível em: https://ntnuopen.ntnu.no/ntnu-xmlui/handle/11250/256570

[9] K. Khosravi, S. Vamegh E., e R. Dhaouadi, "Energy management and control of a standalone PV system using ultracapacitors", em *2015 4th International Conference on Electric Power and Energy Conversion Systems (EPECS)*, nov. 2015, p. 1–6. doi: 10.1109/EPECS.2015.7368511.

[10] R. R. de Melo, F. L. Tofoli, S. Daher, e F. L. M. Antunes, "Interleaved bidirectional DC–DC converter for electric vehicle applications based on multiple energy storage devices", *Electr. Eng.*, vol. 102, nº 4, p. 2011–2023, dez. 2020, doi: 10.1007/s00202-020-01009-3.

[11] H. Ardi, A. Ajami, F. Kardan, e S. Nikpour, "Analysis and Implementation of a Non-Isolated Bidirectional DC-DC Converter with High Voltage Gain", *IEEE Trans. Ind. Electron.*, p. 1–1, 2016, doi: 10.1109/TIE.2016.2552139.

[12] "Ultra-Capacitors in Power Conversion Systems: Applications, Analysis, and Design from Theory to Practice | IEEE eBooks | IEEE Xplore". Acesso em: 21 de julho de 2024. [Online]. Disponível em: https://ieeexplore.ieee.org/book/6670812

[13] J. Ma *et al.*, "The 2021 battery technology roadmap", *J. Phys. Appl. Phys.*, vol. 54, nº 18, p. 183001, fev. 2021, doi: 10.1088/1361-6463/abd353.

[14] M. E. Şahin, F. Blaabjerg, e A. Sangwongwanich, "A Comprehensive Review on Supercapacitor Applications and Developments", *Energies*, vol. 15, nº 3, Art. nº 3, jan. 2022, doi: 10.3390/en15030674.

[15] P. Thounthong, S. Rael, e B. Davat, "Analysis of Supercapacitor as Second Source Based on Fuel Cell Power Generation", *IEEE Trans. Energy Convers.*, vol. 24, nº 1, p. 247–255, mar. 2009, doi: 10.1109/TEC.2008.2003216.

[16] "PSIM User's Manual".

[17] M. K. Kazimierczuk, *Pulse-width Modulated DC–DC Power Converters*.

VI. BIOGRAPHIES
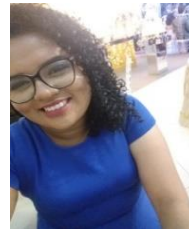
Jessica Cristina Araujo de Sousa was born in Belém – Pará – Brazil, on October 11, 1994. She graduated from the Federal University of Pará (UFPA) – Brazil, in electrical engineering. Currently, she is a master's student in the Postgraduate Program in Electrical Engineering at the Federal University of Pará, in Brazil, in the area of electrical power systems. Her main research interests are power electronics, energy efficiency, distributed generation, and renewable energies.

Thiago Mota Soares was born in Belém – Pará – Brazil on February 21, 1985. He graduated from the Federal University of Pará (UFPA)—Brazil, in electrical engineering and obtained a MSc in electrical power systems from the Federal University of Pará. He is a PhD student and an electrical engineer at the Federal University of Pará, and his main interests in research are power quality issues, energy efficiency, distributed generation, and renewable energies.

Jonathan Muñoz Tabora was born in Santa Rosa de Copán, Honduras 1993. He graduated from the National Autonomous University of Honduras (UNAH) and holds a Ph.D. in Energy Systems focusing on Power Electrical Systems from the Federal University of Pará (UFPA). Currently, he serves as a professor at UNAH. Dr. Muñoz Tabora has knowledge of Motor Drive Systems, Energy Efficiency, Power Quality, Electric Mobility, Electrical Power Systems, and Renewable Energies. He is actively involved in two research and development (R&D) projects related to Energy Efficiency and Microgrids. Additionally, he is the head of the commission of specialists for implementing Minimum Energy Performance Standards (MEPS) for electric motors in Honduras.

Maria Emília De Lima Tostes was born in Recife, Brazil, in 1966. She received the B.Sc., M.Sc., and Ph.D. degrees from the Federal University of Pará, Belém, Brazil, in 1988, 1992, and 2003, respectively. She is currently a Professor with the Electrical and Computer Department, Federal University of Pará. Her main research areas are power quality, distribution systems, and industrial processes